

CELLULAR MECHANISMS OF SEQUENTIAL PROCESSING IN FRONTAL REGIONS REVEALED USING A COMBINED COMPUTATIONAL-fMRI METHODOLOGY

Bickle J¹, Holland SK², Avison MJ³, Schmidthorst, V²

¹Neuroscience Graduate Program, University of Cincinnati, Cincinnati, OH, USA

²Imaging Research Center, Children's Hospital Medical Center, Cincinnati, OH, USA

³Department of Neurology, University of Kentucky Medical Center, Lexington, KY, USA

bicklejw@email.uc.edu holland@athena.chmcc.org avison@mri.uky.edu
vince@athena.chmcc.org

Summary

Here we report preliminary results produced by a combined methodology employing biologically realistic computational modeling and fMRI. Previously we developed a model of frontal cortex saccade command circuitry; here we report how the model computes a sequence of simulated eye movements from an initial fixation point. To produce this realistic performance, however, we had to make some computational assumptions that cannot yet be discharged biologically. When we treat these assumptions as predictions about novel cell and circuitry properties, we can test their plausibility using fMRI on a series of increasingly complex saccade tasks. Preliminary fMRI results confirm some of these predictions and yield new biological data to incorporate into the model. We also present a more extensive set of experiments that will exploit further the interaction of these two methodologies that up until now have been pursued mostly independently of each other. Numerous cytoarchitectural similarities exist between the frontal saccade command regions modeled and imaged here and other frontal cortical regions known to subserve higher cognitive processes. Our neurocomputational model, derived initially from cell properties and anatomy and rendered increasingly biologically plausible by these imaging results, provides plausible and testable hypotheses about the cellular mechanisms underlying sequential processing in cognition and consciousness generally.

Introduction

Neurophysiological background

Neuropsychologists have known for some time that many "higher" cognitive processes are subserved by frontal cortical regions in the primate brain. These include language production, complex motor sequencing, planning, problem solving, and probably even consciousness. However, understanding *how* frontal neurons and circuitries carry out these processes has proven

daunting. Neurocomputational modeling is emerging as a useful technique for formulating hypotheses about these mechanisms. When properly constrained by known cell-physiological and anatomical details, computational models can synthesize lower-level mechanisms with higher-level (behavioral) observations. Owing to their mathematical nature, these models are usually easy to implement on computer simulations. These simulations permit analyses that go beyond existing “wet lab” technology.

To get anything approaching realistic performance in modeled neurons or networks, all serious computational models inevitably go beyond available physiological and anatomical data. This need not be a fatal drawback, however, if we treat these additional assumptions as *predictions* about novel cell properties and anatomical connections in the system being modeled: predictions that can then be tested in the real system using appropriate anatomical, physiological, or imaging techniques. This treatment goes a long way toward addressing the popular worry that computational neuroscience is “not falsifiable.”

To develop a neurocomputational model of frontal “cognitive” processing, it is helpful to find a tractable neural system whose outputs resemble cognitive processes in significant ways. We have found such a system in the frontal saccade command circuitry. Saccades are a type of rapid eye movement that locate the fovea on salient features of a visual stimulus. Humans and nonhuman primates saccade on average 3-5 times per second. Most are executed “involuntarily,” but saccades can be controlled both “voluntarily” and consciously. The primate saccade control system involves both frontal and posterior parietal cortical regions. These regions receive afferents from the dorsal visual stream and project saccade command messages to midbrain, brain stem, and neostriatum sites. The frontal cortical area prominent in generating purposive saccades is the frontal eye fields (FEFs) in premotor cortex, encompassing Brodmann’s area 8a in humans.

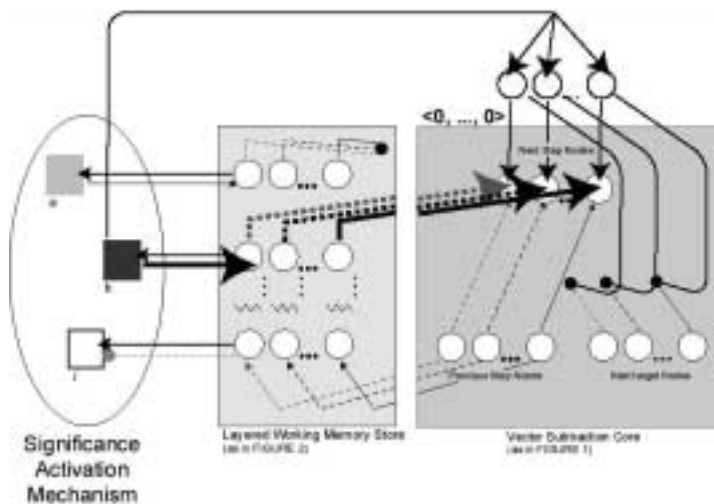
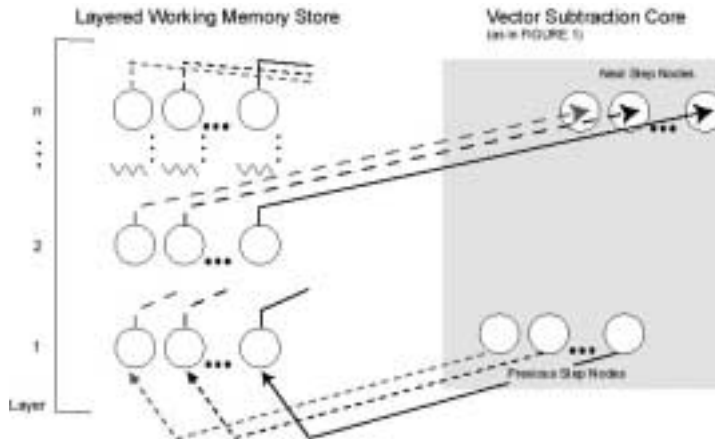
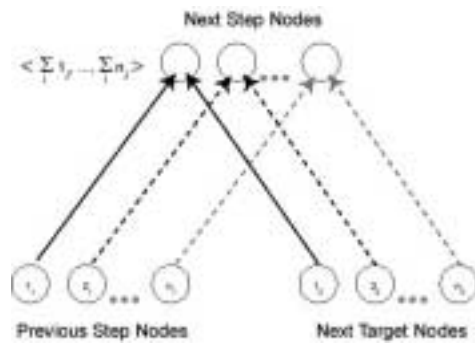
The role of FEFs in saccade command has been studied comprehensively in nonhuman primates at the level of single cell electrophysiology (Bruce and Goldberg 1985; Goldberg and Bruce 1990). FEFs contain both pre- and post-saccadic neurons. The physiological activity and intra-FEF connections between the various neuron types suggest that FEFs implement *vector subtraction* to compute the dimensions of short sequences of saccades from an initial fixation point. This is a nontrivial computational problem, because the dimensions of the second saccade in “eye movement” space are quite different after the first saccade than they would be from the initial fixation point. The single-cell results suggest that FEFs have the resources to compute saccade sequences “on the fly” (“ballistically,” without the need for “reflective feedback”) based on the retinotopic locations of the two stimuli from the initial fixation point and the “eye movement” dimensions of the first saccade. Both pieces of information are encoded and combined in the joint activity of FEF neurons. Most intriguing from a modeling perspective is a class of FEF neurons that have both pre- and post-saccadic movement fields. These cells were most active after saccades *of the opposite direction and amplitude* as their preferred pre-saccadic dimensions (Goldberg and Bruce 1990).

Saccade sequences involving more steps can be computed by FEF neurons so long as the dimensions of earlier saccades in the sequence are held “on line” in working memory. Two candidate areas for saccade-related working memory have been discovered. Goldman-Rakic and her colleagues’ work on the “memory fields” of single neurons in area 46 of dorsolateral prefrontal cortex (DLPFC) is well-known (e.g., Funahashi, Chafee, and Goldman-Rakic 1993). More recently, Courtney *et al.* (1998) have used fMRI to study a proposed “working memory” region more proximal to human FEFs, which have moved posterior and superior relative to their location in rhesus monkey.

Physiological and imaging work in two other regions suggests that they have a role in computing the dimensions of saccade sequences. When properly motivated, humans and nonhuman primates can quickly saccade back to a fixation point after being distracted or prompted to attend to a peripheral stimulus. The anterior cingulate cortex (ACC) appears to be involved in motivated aspects of saccades. Gaymard *et al.* (1998) studied saccade deficits in two patients that structural MRI revealed to share ACC lesions in the posterior portion of the rostral cingulate zone. Both were deficient in tasks requiring either active disengagement from a fixation point or intentional, purposive saccades (memory-guided, previously conditioned without a visual stimulus, and “antisaccades” away from a visual stimulus). They dubbed this region the “cingulate eye fields.” Second are “suppression site” neurons in the FEFs (Burman and Bruce 1997). When these neurons are microstimulated, monkeys’ saccades are delayed until microstimulation ceases and then consistently hypometric (short of target). Their anatomical locations in FEF cortical columns and foveal receptive fields suggested to Burman and Bruce that they code for saccades of 0° amplitude and direction from fixation.

A neurocomputational model that computes the dimensions of saccade sequences

Using these biological details directly to derive computational architecture and parameters, we (Bickle, Worley, and Bernstein 2000; Bernstein, Stiehl, and Bickle 2000) developed a neurocomputational model and subsequent computer simulation that computes the dimensions of multiple saccade sequences from an initial fixation point (Figure 1). The *Vector Subtraction Core* derives from the pre- and post-saccadic activity in FEF neurons. The *Working Memory Store* holds dimensions of early saccades in the sequence on line. It projects this information back into the units in the *Vector Subtraction Core* that compute the dimensions of the next saccade. Its activity derives from neurons with “working memory” fields. Finally, the *Significance Activation Mechanism* (SAM) has a variable activation threshold that when activated inhibits the *Next Target Nodes* in the *Vector Subtraction Core*. This replaces those dimensions with a 0° saccade message. In combination with activity in the *Previous Move Nodes* in the *Vector Subtraction Core* and the *Working Memory Store*, the system computes the dimensions of a saccade that will return it to the initial fixation point from any target in the sequence. SAM and its variable threshold derive from the known physiology and anatomy of the ACC and FEF suppression sites.



Biological plausibility and potential generalizability of the model

Each component of our neurocomputational model and computer simulation of the frontal saccade command circuitry derives directly from cell-physiological and anatomical features, *where these features are currently known*. Our modeling project falls squarely within computational neuroscience. We are not doing abstract network modeling.

The potential significance of a biologically plausible model of saccade sequencing goes beyond vision science. Vector subtraction implemented neurally is potentially a mechanism for sequential processing generally: a hallmark of much higher cognition.

Cytoarchitecturally—in terms of cell types, columnar structure, and cell distributions across both cortical layers and columns—both human and nonhuman primate FEFs consist of typical frontal-type cortex with distinctive granule layers (Parent 1996).

Hence much of frontal cortex known to subserve “higher cognition” shares the cellular makeup of the FEFs. Verifying the biological plausibility of our model for the FEFs suggests that vector subtraction could be a common neural mechanism for computing sequential trajectories through vector spaces generally. Much theoretical neuroscience recommends the potential of treating neural representations as points in high-dimensional vector spaces and neural computations as transitions (trajectories) from points to points (Churchland and Sejnowski 1992). The case for our model’s generalizability to other frontal regions is strengthened by Courtney *et al.*’s (1998) observation that the human FEFs and possibly saccade-related working memory sites have moved posterior and superior to their relative locations in nonhuman primates. This evolutionary shift was presumably to accommodate other cognitive functions subserved by the more anterior and inferior regions of human frontal cortex: presumably by cell types and mechanisms *already implemented* at these sites. Any additional empirical evidence that strengthens the biological plausibility of our model also strengthens its potential as a general cellular mechanism for sequential cognitive processing across frontal cortex.

Computation assumptions and the potential of fMRI to test them

In order to get realistic performance out of our model and computer simulation, we were forced to make numerous computational assumptions that we could not discharge biologically. This is a common problem for current modeling projects that derive their architectural and computational parameters from extant neurophysiology and anatomy. Prominent among the assumptions we made is the order in which activity occurs in the neural regions modeled—FEFs, frontal spatial working memory areas (SWM), and ACC—as saccade tasks increase in complexity. Our model predicts that saccade-related activity in a simple two-step task is restricted to FEFs. According to the model, FEFs contain resources (pre- and post-saccadic neuronal “movement fields”) sufficient to compute the dimensions of both saccades in the sequence. As saccade tasks grow in complexity to three-step sequences, the model predicts activity in both the FEFs and SWN regions. The latter is assumed necessary to hold “temporarily on line” the dimensions of the post-saccadic activity generated by the first saccade in the sequence. The model also predicts an increase in the level of FEF activity. More information is streaming into the FEFs to compute the dimensions of the third saccade (from both the dorsal visual stream and frontal SWM regions). Finally, saccade tasks that involve a four-step sequence (with visual stimuli presented within 100 msec of one another) appear to tax the human SWM storage capacity. Our model predicts that activity in the ACC will show up on this task (in addition to activity in FEFs and frontal SWM sites) to handle a motivated saccade back to initial fixation point when the subject’s performance breaks down.

Our model leaves other biological questions open. Where is the site of SWM: area 46 in DLPFC or the more posterior and superior areas suggested by Courtney *et al.* (1998)? Does the ACC play a “central executive” monitoring role during saccade sequencing or is it rather “called in to the rescue” after the SWM

store gets overloaded? With each empirical answer to such questions, we can refine our neurocomputational model and computer simulation to better reflect the actual timing and intensity of each component in the saccade sequencing command circuit: thereby increasing its biological plausibility.

Functional magnetic resonance imaging (fMRI) based upon “Blood Oxygen Level Dependent” (BOLD) contrast has emerged over the last decade as a powerful tool for noninvasive investigations of human brain activation patterns (Ogawa *et al.* 1990; Kwong *et al.* 1992). BOLD-fMRI is now widely used by neuroscience researchers (Sanders and Orrison 1995) as a tool for studies of somato-sensory function, neurocognitive processes, learning, memory, and attention. In this context fMRI has been used extensively to visualize such patterns, both normal and pathological, associated with vision, hearing, language, and higher order cognitive functions. Coupled with appropriate behavioral tasks, this method is ideally suited to test our neurocomputational model’s assumptions-cum-predictions about order of activation and activity intensity in frontal saccade sequencing command regions.

The advantages of combining neurocomputational modeling with fMRI don’t flow in only one direction. fMRI has yet to transcend a neo-phrenology status among neuroscience researchers and demonstrate its full potential for investigations of the mind. Computational modeling can provide a connection between the underlying biological processes and brain activation patterns revealed by fMRI. Conversely, fMRI can provide new observations to guide focused and relevant refinements toward more realistic computational models of human cognition. Single cell measurements cannot do this readily. Clearly, this is a combined methodology worth pursuing for the benefit of both techniques.

Our hypotheses and specific aims

Underlying the preliminary data reported below is an overarching hypothesis that a neurobiologically plausible computational model of visual saccade processing can predict the patterns of cortical activation observed in humans by fMRI. In the studies we have carried out so far, we address the following sub-hypotheses:

- fMRI allows us to identify cortical sites of saccade-associated activity which are the functional homologues of specific modules of the computational model
- The order in which specific brain regions are activated (as revealed by fMRI) as a function of increasing complexity of the saccade task reflect the information flow between the modules within the computational network.
- Strengths of saccade-associated activations measured by fMRI reflect the computational/synaptic activity of the equivalent modules in the computational model and can be used to validate and refine the model.

In order to test these hypotheses, we are pursuing the following specific aims:

1. In normal human subjects, use fMRI to characterize the sites of cortical activation associated with performance of a range of saccade tasks that differentially engage key elements of the saccadic network (FEFs, SWMs, ACC).
2. For a range of saccade conditions, compare the sites, levels, order, and time of onset of cortical activation with those predicted by the computational model.
3. In an iterative manner, use the fMRI results to refine the computational model, extending the model's biological plausibility.

Methods

Experiments with Sequential Inputs to the Computer-Simulated Neurocomputational Model

We have presented sequences of targets to our computer-simulated neurocomputational model to demonstrate its capacity to compute the dimensions of multiple steps through simulated “eye movement” space and to return to the original fixation point from any point mid-sequence when the SAM component is activated.

fMRI Studies of Visually Guided Saccades

Our neurocomputational model described above makes predictions about changes in levels of activity in FEF, SWM, and ACC associated with changes in the “saccade burden”. Preliminary fMRI studies were designed to (1) identify frontal cortical areas previously identified as FEF, SWM and ACC; (2) obtain preliminary data addressing the hypothesis that the levels of activation in one or more of these areas is modulated by the “saccade burden” in a manner consistent with the predictions of the computational model.

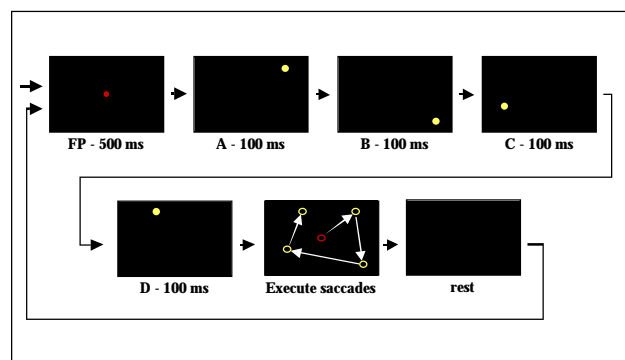
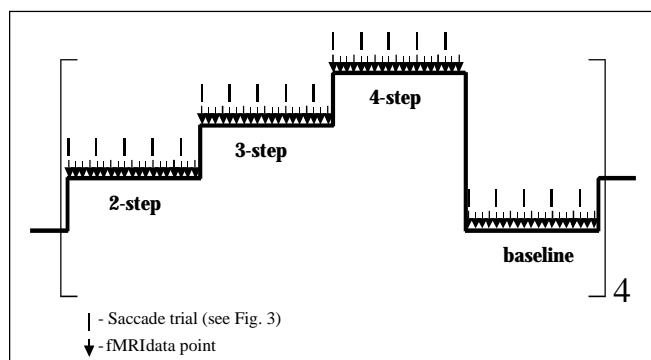


Table 1 – Timing of dot patterns for block periodic visual saccade fMRI paradigm

**2 step saccade block - 5 presentations
30 seconds**

500 msec	fixation point
100 msec	1 st dot
100 msec	2 nd dot
5300 msec	black screen

**3 step saccade block - 5 presentations
30 seconds**

500 msec	fixation point
100 msec	1 st dot
100 msec	2 nd dot
100 msec	3 rd dot
5200 msec	black screen

**4 step saccade block - 5 presentations
30 seconds**

500 msec	fixation point
100 msec	1 st dot
100 msec	2 nd dot
100 msec	3 rd dot
100 msec	4 th dot
5100 msec	black screen

Control Block - 30 seconds

Subjects: fMRI studies were performed in a cohort of healthy adults, all of whom gave informed consent under a protocol approved by the Institutional Review Board of Childrens' Hospital Medical Center.

Saccade Tasks: Subjects executed four cycles of blocks of 2-, 3-, and 4-step saccades, and a baseline sensory-motor task (Figure 2). Table 1 summarizes the timing of presentation for each saccade condition, while Figure 3 illustrates the nature of the visual target stimuli presented during the saccade tasks. The general structure of each saccadic trial was as follows: a trial began with presentation of a centrally located red fixation point (FP) against a black background for 0.5 seconds. After 0.5 seconds the central red dot extinguished and was followed immediately by a sequence of 2, 3, or 4 yellow dots, each dot positioned at randomly generated locations in one of 8 octants and one of 2 radial distances from the center. Each yellow dot appeared for 100 msec against the same black background, and after the final yellow dot was extinguished, a black screen was presented until the duration of

the entire trial (6.0 seconds). Each trial was repeated 5 times within a block, for a block duration of 30 seconds, and a cycle duration of 2 minutes. For each trial, the subject was instructed to fixate on the red dot initially, and when the yellow dots appeared, to saccade from one target to the next in the correct order of presentation. Due to the short (100ms) duration of each target presentation, the target to be saccaded to had extinguished prior to saccade initiation. Thus as the number of targets increased, task execution made increasing demands on working memory (particularly for the 3- and 4-step saccades). By the 4-step task, subjects reported difficulty in task execution. This suggested the limits of working memory, a condition under which ACC activation ("central executive" monitoring versus "rescue call" response) can be probed. The task stimuli were presented using an MRI compatible audiovisual system (Resonance Technologies Inc., Van Nuys, CA).

We used a bilateral finger-tapping task as the control condition. The sensory-motor response to bilateral finger tapping has been investigated extensively in the clinical literature and in previous studies of pediatric epilepsy patients (Holland *et al.* 1999). We instructed subjects to tap their fingers

sequentially to the thumbs on both hands simultaneously each time a green dot appeared on the screen (at the beginning of the control block). The sequential tapping rate was self-paced and we instructed subjects to stop after touching each finger to their thumb twice. This control task distracts subjects from the saccade task during the control period and provides activation of the motor strip as reference data for each subject. In the absence of eye tracking capabilities, this task also provided observable confirmation of compliance with the task.

The MRI compatible audiovisual system presenting task stimuli is equipped with a high-quality pneumatic headphone that administers audio instructions to subjects and provides up to 30dB of sound isolation from MRI scanner noise. In the absence of eye-tracking capabilities, we assessed task performance by each subjects' post-study self-report.

Each fMRI study comprised four cycles plus an additional baseline block at the beginning, for a total study duration of 8.5 minutes.

FMRI: We acquired activation data at 3T using BOLD-sensitized T2*-weighted, gradient-echo EPI (TR/TE= 1500/38 msec). Twenty-four slices were acquired at 340 time points during the sequential 30-second saccade blocks and control behavior for a total imaging time of 8 min. 30 sec. The initial 20 time points (corresponding to the first block of baseline data) were discarded to ensure steady-state magnetization subject's habituation to the scanner. We performed a 3D MDEFT (Modified Driven Equilibrium Fourier Transform) whole brain scan in an axial plane (Ugurbil *et al.* 1993; Duewll *et al.* 1996) to provide high-resolution anatomical images to coregister activation maps and structural normalization to Talairach space. Acquisition parameters were: TR/TE/ = 15.7/4.3/550 msec, FOV=25.6 x 19.2 x 19.2 cm, matrix = 256 X 128 X 128, total imaging time, approximately 9 minutes. This scan yields 3D resolution of 1 x 1.5 x 1.5 mm and provides excellent anatomical resolution and contrast between gray matter and white matter in the brain (Wansapura *et al.* 1999; Holland *et al.* 2001).

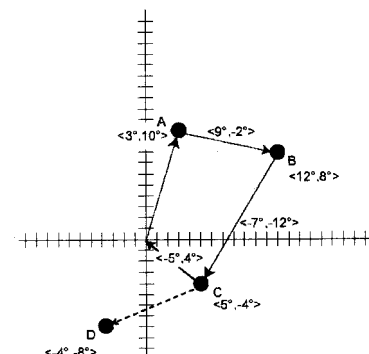
FMRI Post-processing: Post-processing was done using Cincinnati Children's Hospital Image Processing Software (CCHIPS[®]) (Schmithorst and Dardzinski 2000) developed in the Imaging Research Center at Children's Hospital Medical Center in the IDL[®] software environment (Research Systems Inc., Boulder, CO).

For our present activation paradigm, cross-correlation between the BOLD signal intensity time-course and the reference function illustrated in Figure 2 was performed for each subject on a pixel-by-pixel basis. Pixels above a statistically appropriate correlation threshold were overlaid on a coregistered anatomical image acquired at the same time. In this manner we computed activation maps for each subject. These statistical parametric maps were then transformed into Talairach space for composite analysis (Talairach and Tournoux 1988). These correlation maps were averaged across all subjects and a composite activation map based on the average correlation value for all subjects could then be displayed for each comparison.

Results

- Sequential processing in the neurocomputational model and computer simulation

Figure 4 illustrates the combined workings of all components of our neurocomputational model and computer simulation, transduced into behavioral (eye movement) parameters. (The x-axis reflects degrees of horizontal eye movement from fixation point FP. The y-axis reflects degrees of vertical eye movement from FP.) First target A in the sequence produces a vector $\langle 3, 10 \rangle$ in the Next Target Nodes and $\langle 0, 0 \rangle$ in the Previous Step Nodes of the Vector Subtraction Core. (The latter value owes to the fact that this is the first saccade in the sequence.) This yields a vector of $\langle 0+3, 0+10 \rangle = \langle 3, 10 \rangle$ in the Next Step Nodes. The system then executes a saccade of these dimensions in simulated eye movement space, landing on target A. Second target B in the saccade sequence then produces a vector $\langle 12, 8 \rangle$ in the Next Target Nodes while a vector $\langle -3, -10 \rangle$ obtains in the Previous Step Nodes. (The latter is the opposite dimensions of the saccade just executed, in keeping with the physiological discoveries of post-saccadic movement fields in FEF neurons.) This yields a vector $\langle -3+12, -10+8 \rangle = \langle 9, -2 \rangle$ in the Next Step Nodes. The system executes a saccade of these dimensions, reaching target B from A.



This yields a vector of $\langle 0+3, 0+10 \rangle = \langle 3, 10 \rangle$ in the Next Step Nodes. The system then executes a saccade of these dimensions in simulated eye movement space, landing on target A. Second target B in the saccade sequence then produces a vector $\langle 12, 8 \rangle$ in the Next Target Nodes while a vector $\langle -3, -10 \rangle$ obtains in the Previous Step Nodes. (The latter is the opposite dimensions of the saccade just executed, in keeping with the physiological discoveries of post-saccadic movement fields in FEF neurons.) This yields a vector $\langle -3+12, -10+8 \rangle = \langle 9, -2 \rangle$ in the Next Step Nodes. The system executes a saccade of these dimensions, reaching target B from A.

At this point the Working Memory Store comes into play, storing the dimensions of post-saccadic activity produced by the first saccade in the sequence: $\langle -3, -10 \rangle$. This value is projected to the Next Step Nodes of the Vector Subtraction Core, along with vectors $\langle -9, 2 \rangle$ in the Previous Step Nodes (the opposite dimensions of the saccade just executed) and $\langle 5, -4 \rangle$ (generated in the Next Target Nodes by the third target C in the sequence). The Next Step Nodes compute the dimensions of the next saccade: $\langle -3+-9+5, -10+2+-4 \rangle = \langle -7, -12 \rangle$. The system executes a saccade of these dimensions, reaching target C from B.

If the system continues with the sequence to compute the saccade dimensions from C to D (dotted line in Figure 2), the Working Memory Store contributes the post-saccadic dimensions of the first two saccades: $\langle -3, -10 \rangle$, $\langle -9, 2 \rangle$. The Previous Step Nodes now contain the dimensions of the post-saccadic activity elicited by the saccade just executed: $\langle 7, 12 \rangle$. The Next Target Nodes contribute the dimensions of Target D from the original origin: $\langle -4, -8 \rangle$. So the Next Step Nodes compute a saccades command with dimensions $\langle -3+-9+7+-4, -10+2+12+-8 \rangle = \langle -9, -4 \rangle$. The system executes a saccade of those dimensions, reaching target D from C. But if the Variable Threshold controlling SAM activation is set at the second layer of the Working Memory Store, the Return to Origin mechanism inhibits the projection of the Next Target to the Next Step Nodes, replacing the vector $\langle -4, -8 \rangle$ in the above calculation with $\langle 0, 0 \rangle$. This change yields a saccade command with dimensions $\langle -3+-9+7+0, -10+2+12+0 \rangle = \langle -5, 4 \rangle$. The system executes a saccade with these dimensions, returning to the initial fixation point from target C (solid line in Figure 2 above).

- Identification of FEF, SWM and ACC Using FMRI

To identify those frontal cortical regions subserving saccade activity, we adopted two strategies. First, we identified those regions that were significantly activated during periods of saccade activity in any of the contrasts with the control sensory-motor task. Second, we identified those voxels in the grouped data in which the amplitude of the BOLD-sensitized fMRI signal was significantly correlated ($p < 0.01$) with the number of saccade steps per trial (i.e. increasing “saccade burden”). These strategies clearly identified the FEF, ACC, and regions of frontal lobe, including those previously associated with working memory functions in humans.

The location of a dedicated spatial working memory area (and indeed its very existence) remains unclear, but our data clearly show activation of several candidate areas. We discuss one particular area previously identified by Courtney et al. (1998) in more detail below.

Figure 5 shows the results of the second approach, namely a pixel-by-pixel correlation between the MRI signal and number of saccade steps. The correlation value was transformed into a t-statistic and averaged across all subjects. Pixels which exceeded a significance of $p < 0.01$ were then overlaid across the averaged anatomical dataset.

- Relation of FEF activation to “Saccade Burden”

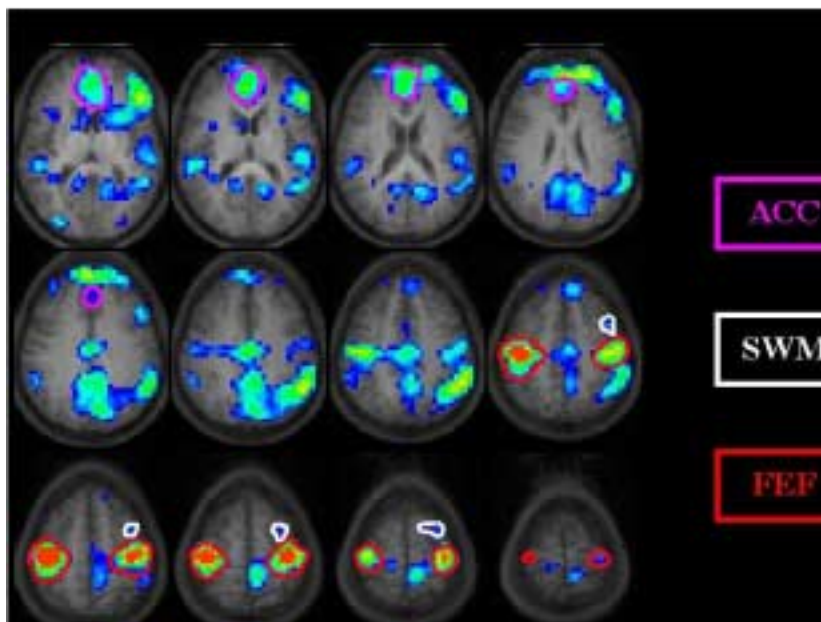


[Figure 5 – Activation map showing those regions exhibiting significant \(\$p < 0.01\$ \) correlation of BOLD-sensitized fMRI signal amplitude with saccade burden. Candidate regions for functional homologues of the computational modules are frontal eye fields \(FEF, red outline\), spatial working memory \(SWM, white\), anterior cingulate cortex \(ACC, purple\).](#)

One prediction of the model as implemented, is that the computational demands on the FEF will scale monotonically with increasing number of saccades to be executed. Figure 6 (left) plots the mean BOLD signal amplitude in the FEF of one of the six volunteers during execution of 2-, 3-, and 4-step saccades. Consistent with the model’s prediction, the increase in BOLD signal amplitude when increasing the saccade burden from 3- to 4-step saccades is the

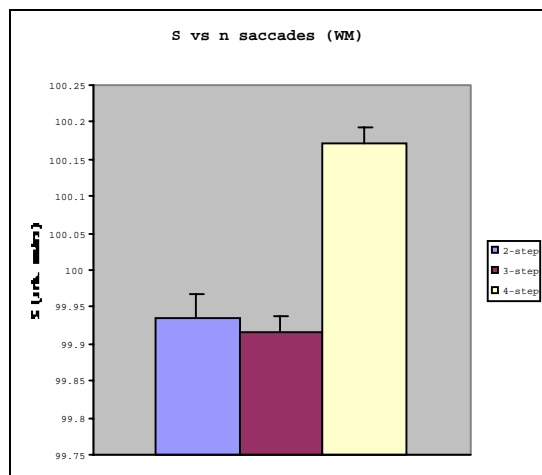
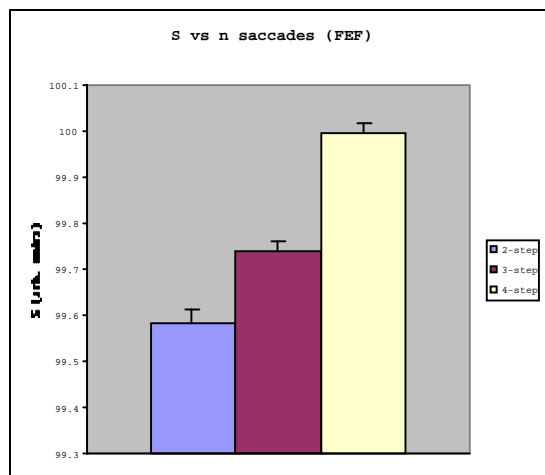
same as the increase observed when increasing the burden from 2- to 3-step saccades.

In contrast, the behavior of a cortical region we have tentatively identified as the spatial working memory module described by Courtney *et al.* (1998), exhibits no increase in activity between the 2- and 3-step conditions, but shows a significant increase between the 3- and 4-step conditions (Figure 6 right). Interestingly, the activity during the 2- and 3-step saccade conditions is not significantly different from that under baseline conditions. This suggests that the FEF may itself maintain an active working memory, whose capacity is only exceeded when the number of saccades to be executed is greater than 3.

Conclusions

Our preliminary fMRI results suggest that some of our model's assumptions, treated as novel physiological predictions about the order and amount of activity in various regions of the primate saccade circuitry, are correct. The FEFs do appear to be the only region of the saccade circuitry activated during the two-step task, and activity within this region seems to scale monotonically with increasing task complexity. The ACC is active when task demands exceed working memory capacity (in the four-step saccade task). But the FEFs also seem to contain (limited) resources for holding "on line" the dimensions of earlier saccades beyond those needed to compute the dimensions of the second saccade in the sequence: at the very least, our preliminary data suggests that frontal regions for saccade working memory become active during the four-step saccade task. If this result is verified within a comprehensive study, our combined neurocomputational modeling—fMRI study will have yielded a novel insight about saccade command generation. Revising our neurocomputational model to accommodate such a result while still producing realistic saccade command outputs might require further assumptions that go beyond existing anatomical and physiological knowledge. These assumptions too can be treated as predictions for further experimental studies.

This is just a single example of results we expect our combined neurocomputational modeling—fMRI studies to reveal. We have now designed an experiment that will tease out the roles of the different frontal "spatial working



memory” areas in sequential saccade generation. Only a 3-step saccade task will be alternated with the control interval task. fMRI will be performed in 24 slices as described above. However, in this series the time interval between the appearance of the final saccade target and the go signal (disappearance of the central red fixation point) will vary from zero to 500 msec to 1500 msec in each 30 second block of the 4-block cycle. As demonstrated by Courtney *et al.* (1998), computations involving “fast” working memory saccade functions may be performed in a region adjacent to the FEF. Consistent with this view, Gaymard *et al.* (1999) demonstrated a loss of short-term spatial working memory in a patient with a lesion restricted to FEF and not involving DLPFC. A different role for DLPFC in longer-term working memory is suggested by transcranial magnetic stimulation studies of Muri *et al.* (1996) and Brandt *et al.* (1998). Therefore we predict that only posterior spatial working memory areas near the FEF will be engaged by the saccade sequence involving the 500 msec delay. On the other hand, for the longer delay of 1500 msec, the DLPFC will be more strongly activated as information will have time to flow to this location for true working memory storage. Validation of this modification to the biological circuitry for saccades based upon monkey single-cell data could have profound implications for the computational model.

We have also designed experiments to test whether the ACC plays a “central executive” monitoring role during saccade sequencing, or rather is “called to the rescue” by an overloaded working memory store during multiple saccade memory tasks. First, we will repeat the fMRI paradigm carried out in the preliminary studies with one modification to the visual stimulation sequence. Subjects will be instructed to return the eyes to the remembered fixation point upon completion of each saccade sequence or upon failing to complete the sequence correctly. As the task difficulty increases with the number of saccade steps, subjects will be expected to fail more frequently. Rather than allow their eyes to wander or to engage in involuntary saccades, they will return to the location of the fixation point. An eye tracker will provide a record of compliance with this instruction. We will compute correlations between number of saccades and levels of activation in each of the regions of interest (ROIs) (FEF, ACC, DLPFC) and determine their significance levels. We will also compute correlations between brain activation and performance as monitored with the eye tracker. This information will be particularly relevant in assessing the role of the ACC as either a monitoring or “rescue” system.

In another study, we will probe the temporal dimension of saccade processing using a rapid sampling event-related fMRI paradigm. We will use the same task design as described in the previous paragraph except that the interval between saccade trials will be increased to 15 seconds to avoid overlap of the hemodynamic responses from sequential trials. We will perform fMRI scans in only two slices, selected based upon the data from the previous experiment to encompass the key ROIs. Images will be acquired at 125 msec intervals from these slices. In this way we aim to measure the time delays in activation between neural components of the saccade circuit, especially area 46 in DLPFC, the SWM area described by Courtney *et al.* (1998) and ACC. Data will be processed

using the Bandettini cross-correlation method (Bandettini et al. 1993) with a variable lag time between the image frames and the reference function. The time delay to maximum correlation in each pixel will be computed and mapped as a color-coded overlay onto the anatomical data. Composite time delay maps will be computed from the data from all subjects to improve power. They will provide a convenient visual display of the temporal relationships between neural components of the saccade network. We will be able to identify faster and slower components of working memory and spatial working memory from this data, as well as the exact time course of ACC activation in tasks where the saccade burden exceeds the system's capacity. Such time-domain information will provide critical new information to guide refinements to our neurocomputational model.

Expansion of the frontal lobes is believed to underlie many of the higher cognitive attributes that distinguish humans from nonhuman primates. The neural circuitry of the human frontal lobes remains poorly understood, however, due in part to the technical limitations of studying brain function in humans, and in part to the difficulty of identifying, characterizing, and relating these higher functions to the underlying circuitry both in humans and in nonhuman primates. The neuroanatomy and cytoarchitecture of the frontal areas subserving saccade activity resemble that found in much of the frontal cortex, suggesting that the cell properties, circuitry and computational strategies of the visual saccade system may generalize to other frontal regions that subserve the more abstract, characteristically human "higher" cognitive functions.

References

- Bandettini PA *et al.*: Processing strategies for time-course data sets in functional MRI of the human brain. *Magnetic Resonance in Medicine* 1993; 30: 161-175.
- Bernstein M, Stiehl S, Bickle J: The effect of motivation on the stream of consciousness: Generalizing from a neurocomputational model of cingulo-frontal circuits controlling saccadic eye movements. In Ellis R and Newton N (eds.) *The Cauldron of Consciousness: Motivation, Affect and Self-Organization*, 2000. John Benjamins: Amsterdam, 133-161
- Bickle J, Worley C, Bernstein B: Vector subtraction implemented neurally: A neurocomputational model of some sequential cognitive and conscious processes. *Consciousness and Cognition* 2000; 9: 117-144.
- Brandt SA *et al.*: Effects of repetitive transcranial magnetic stimulation over dorsolateral prefrontal and posterior parietal cortex on memory-guided saccades. *Experimental Brain Research* 1998; 118: 197-204.
- Bruce CJ, Goldberg ME: Primate frontal eye fields. I. Single neurons discharging before saccades. *Journal of Neurophysiology* 1985; 53: 603-635.
- Burman D, Bruce CJ: Suppression of task-related saccades by electrical stimulation in the primate's frontal eye fields. *Journal of Neurophysiology* 1997; 77: 2252-2267.
- Churchland PS, Sejnowski TJ: *The Computational Brain*. 1992. MIT Press: Cambridge, MA
- Courtney S *et al.*: An area specialized for spatial working memory in the human frontal cortex. *Science* 1998; 279: 1347-1351.

- Duewll S *et al.*: MR imaging contrast in human brain tissue: Assessment and optimization at 4T. *Radiology* 1996; 199: 780-786.
- Funahashi S, Chafee M, Goldman-Rakic P: Prefrontal neuronal activity in rhesus monkey s performing an antisaccade task. *Nature* 1993; 753-756.
- Gaymard B *et al.*: Effects of anterior cingulate cortex lesions on ocular saccades in humans. *Experimental Brain Research* 1998; 120: 173-183.
- Gaymard B *et al.*: The frontal eye field is involved in spatial short-term memory but not in reflexive saccade inhibition. *Experimental Brain Research* 1999; 129: 288-301.
- Goldberg ME, Bruce CJ: Primate frontal eye fields. III. Maintenance of spatially accurate saccade signal. *Journal of Neurophysiology* 1990; 64: 489-508.
- Holland SK *et al.*: Normal brain activation patterns in children performing a verb generation task. *Neuroimage* in press.
- Holland SK *et al.*: Differences in fMRI language activation patterns between audio and visual presentation of the same verb generation task in pediatric epilepsy patients. *ISMRM 7th Annual Meeting and Exhibition* 1999; Philadelphia, PA
- Kwong KK *et al.*: Dynamic magnetic resonance imaging of human brain activity during primary sensory stimulation. *Proceedings of the National Academy of Sciences USA* 1992; 89: 5675-5679.
- Muri RM *et al.*: Effects of single-pulse transcranial magnetic stimulation over the prefrontal and parietal cortices during memory-guided saccades in humans. *Journal of Neurophysiology* 1996; 76: 2102-2106.
- Ogawa S *et al.*: Oxygenation-sensitive contrast in magnetic resonance image of rodent brain at high magnetic fields. *Magnetic Resonance in Medicine* 1990; 14: 68-78.
- Parent A: *Carpenter's Human Neuroanatomy*, 9th Ed. Williams and Wilkins: Baltimore.
- Sanders J, Orrison W: Functional magnetic resonance imaging. In Orrison W *et al.* (eds.): *Functional Brain Imaging*. Mosby: St, Louis, 229-236.
- Schmidthorst VJ, Dardzinski BJ: CCHIPS/IDL enables detailed MRI analysis. http://www.researchsystems.com/AppProfile/idl_med_cchips.cfm. 2000.
- Talairach J, Tournoux P: *Co-planar Stereotaxic Atlas of the Human Brain*. Thieme Medical: New York.
- Ugurbil K *et al.*: Imaging at high magnetic fields: Initial experience at 4T. *Magnetic Resonance Quarterly* 1993; 9: 259-277.
- Wansapura JP *et al.*: NMR relaxation times in the human brain at 3.0 Tesla. *Journal of Magnetic Resonance Imaging* 1999; 9: 531-538.